Supporting Information

Layered CrO$_2$·nH$_2$O as cathode material for aqueous zinc-ion batteries: Ab initio study

Lu Liu,[a] Zixi He,[a] Binghan Wu,[a] Hongjia Song,[a]*Xiangli Zhong,[a] Jinbin Wang,[a] Daifeng Zou,[b]

Juanjuan Cheng[b]*

[a]*School of Materials Science and Engineering, Key Laboratory of Low-dimensional Materials and*

Application Technology, Xiangtan University, Xiangtan 411105, P. R. China

[b]*School of Materials Science and Engineering, Hunan Provincial Key Lab of Advanced Materials*

for New Energy Storage and Conversion, Department of Physics and Electronic Science, Hunan

University of Science and Technology, Xiangtan 411201, P. R. China

*Corresponding author e-mail address: hjsong@xtu.edu.cn (Hongjia Song)

jjcheng@hnust.edu.cn (Juanjuan Cheng)
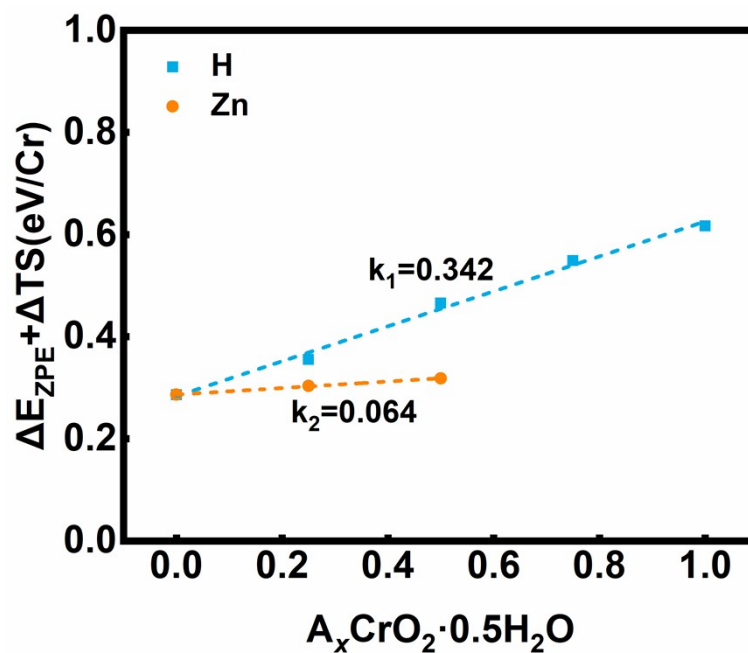
Supplimentary Note1

Fig. S1 The zero vibration energy (ΔE_{ZPE}) and entropy change(ΔS) of $A_xCrO_2 \cdot 0.5H_2O$ at 298.15 K

By comparing the energy added values (zero-point vibration energy (ΔE_{ZPE}) and entropy change (ΔS)) of the $A_xCrO_2 \cdot 0.5H_2O$ (A=H/Zn) structure at 298.15 K, it can be found that the slope corresponding to the H insertion process of the $H_yCrO_2 \cdot 0.5H_2O$ structure is 0.342, indicating that the additional value has a significant impact on H insertion mechanism. The slope of the $Zn_xCrO_2 \cdot 0.5H_2O$ structure during the Zn insertion process is only 0.064, indicating that the added value has a relatively small impact on the Zn insertion mechanism.
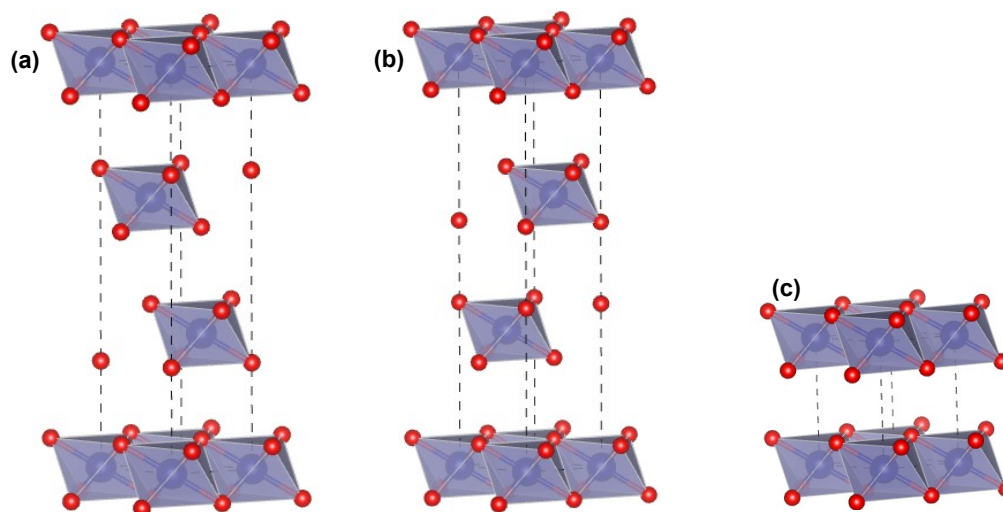
Supplimentary Note1

Fig. S2 Different stacking configurations of layered CrO_2 structures, (a) O3 stacking; (b) P3 stacking; (c) O1 stacking.

Table S1 The lattice parameters of different stacking structures under the interlayer interaction strategy are modified by DFT-D3(U)

Stacking type	Van der Waals	Lattice parameter (Å)		E(meV/f.u.)
O1	DFT-D3(U)	a=b=2.91, c= 4.58	——	-22.079
O3	PBE	a=b=2.92, c=14.90		
	DFT-D3	a=b=2.89, c=13.49		
	DFT-D3(U)	a=b=2.91, c=13.67	a=b=2.8797, c=14.169[1]	-22.085
	vdW-DF2(U)	a=b=2.98, c=13.77		
	opt86b-vdw(U)	a=b=2.91, c=13.48		
P3	DFT-D3(U)	a=b=2.91, c=14.64	a=b=2.8578, c=14.002[2]	-22.048

The common stacking configurations of layered structures include O1, P3, and O3 stacking. The difference between the three structures is the lateral stacking displacement of the O-Cr-O layer, where oxygen atoms exhibit ABAB, ABBCCA, and ABCABC stacking along the c-axis direction, respectively. By using different van der Waals correction methods to correct the interlayer spacing of O3-CrO_2 structure, it was found that the theoretical value was always smaller than the c-axis of the experimentally reported O3-CrO_2 structure, which may be related to the presence of a small amount of Na^+ between the CrO_2 layers ($Na_\delta CrO_2$)[1]. Therefore, the subsequent calculations were only optimized using the DFT-D3 (U) method.

Occupation site

For the Zn insertion mechanism, the non-equivalent sites occupied by Zn are the octahedral center (Zn_1) and tetrahedral center (Zn_2), with corresponding adsorption energies (E_{ad}) of -4.48 eV and -3.98 eV. Meanwhile, for the H insertion mechanism, the non-equivalent sites occupied by H in the O3-CrO_2 structure are lattice oxygen forming -OH bonds and pointing towards the octahedral center (H_1), octahedral center (H_2), and parallel tetrahedral center (H_3), respectively. The corresponding adsorption energies (E_{ad}) are -2.68 eV, 0.38 eV, and -2.39 eV. The non-equivalent sites occupied by H in the P3-CrO_2 structure are the interlayer hydrogen bonding (H_1), tetrahedral center (H_2), and hexagonal prism center (H_3) formed by H and lattice oxygen. The structural optimization of H located at the center of the hexagonal prism has not converged, and the corresponding adsorption energies (E_{ad}) for the latter two are -2.79 eV and 0.45 eV.
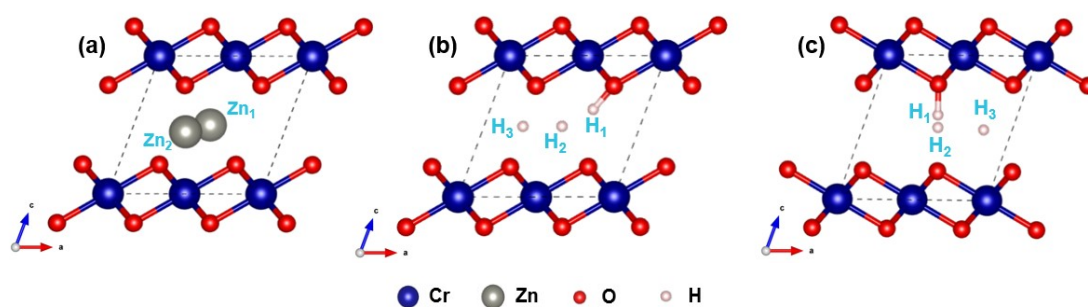

Fig. S3 For different reaction mechanisms, the non-equivalent sites occupied by the guest species in the CrO_2 structure, (a) Zn insertion; (b) H insertion (O3 stacking); (c) H insertion (P3 stacking)
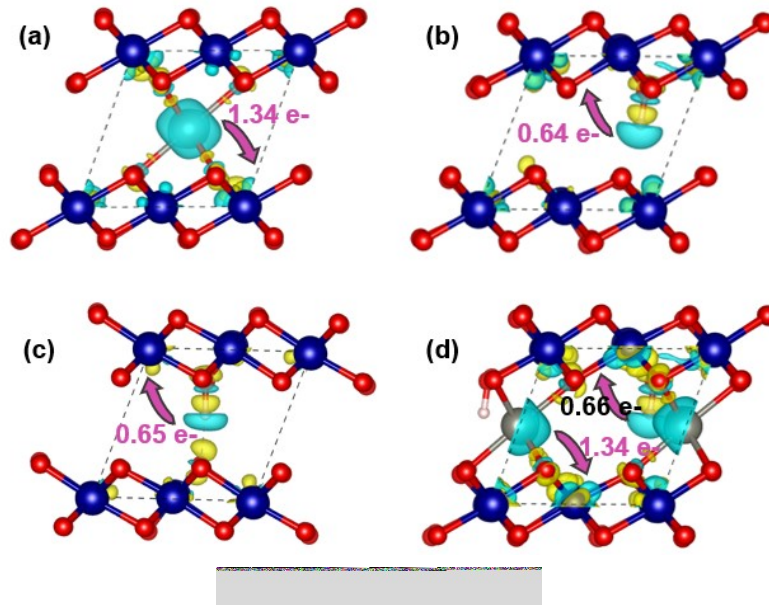
Fig. S4 The charge density differences between the guest ion and the substrate under different reaction mechanisms, (a)$Zn_{0.125}CrO_2$ (Zn insertion); (b)O3-$H_{0.125}CrO_2$(H insertion); (c)P3-$H_{0.125}CrO_2$(H insertion); (d)$H_{0.125}Zn_{0.125}CrO_2$(H/Zn co-insertion). The green and yellow indicate electron depletion and aggregation, respectively，The isosurface is 0.01 electron/ $Å^3$.

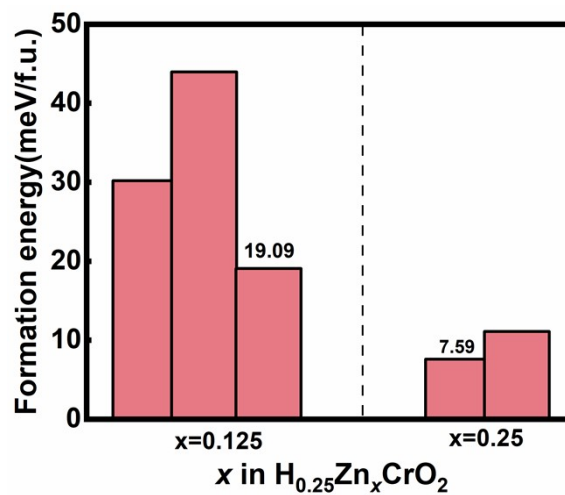Fig. S5 The formation energy of different $H_{0.25}Zn_xCrO_2$ configurations
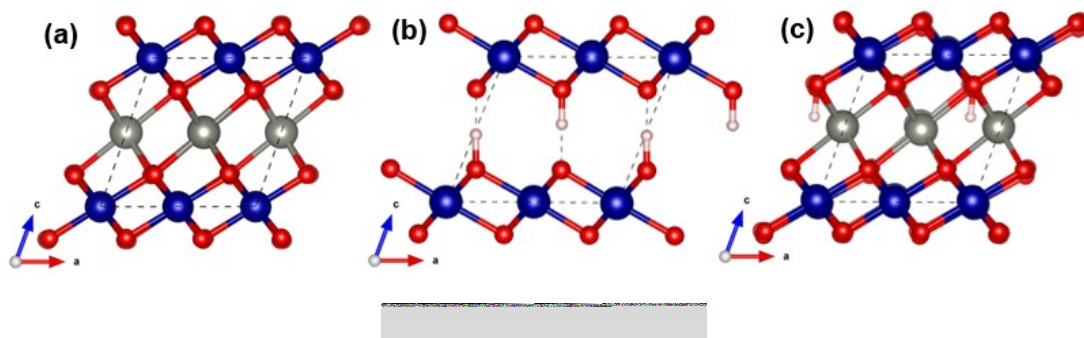
Fig. S6 The theoretical capacity of CrO_2 electrode is based on different reaction mechanisms,(a) $Zn_{0.5}CrO_2$(Zn insertion); (b)P3-$HCrO_2$(H insertion); (c)$H_{0.125}Zn_{0.375}CrO_2$(H/Zn co-insertion).
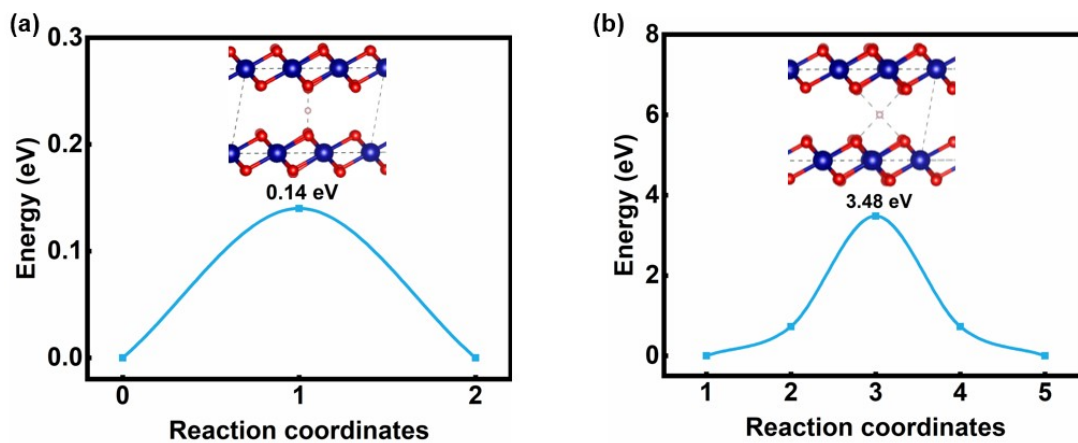
H insertion mechanism

Fig. S7 The diffusion barrier and corresponding transition state model of H in P3-CrO_2 structure (a) Path 1(Longitudinal jump); (b)Path 2(Transverse diffusion)
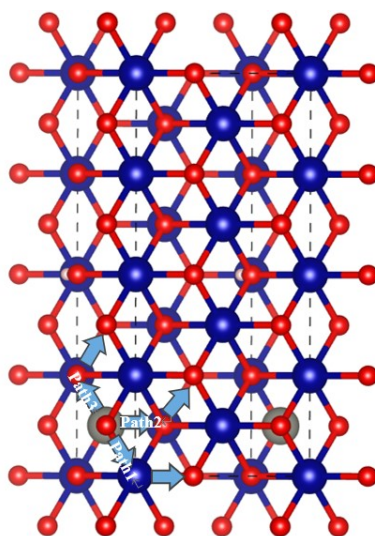
H/Zn co-insertion mechanism

Fig. S8 The three diffusion paths of Zn at the CrO_2 electrode are under the H/Zn co-insertion mechanism

CrO₂·nH₂O (n=0.25~1.0)
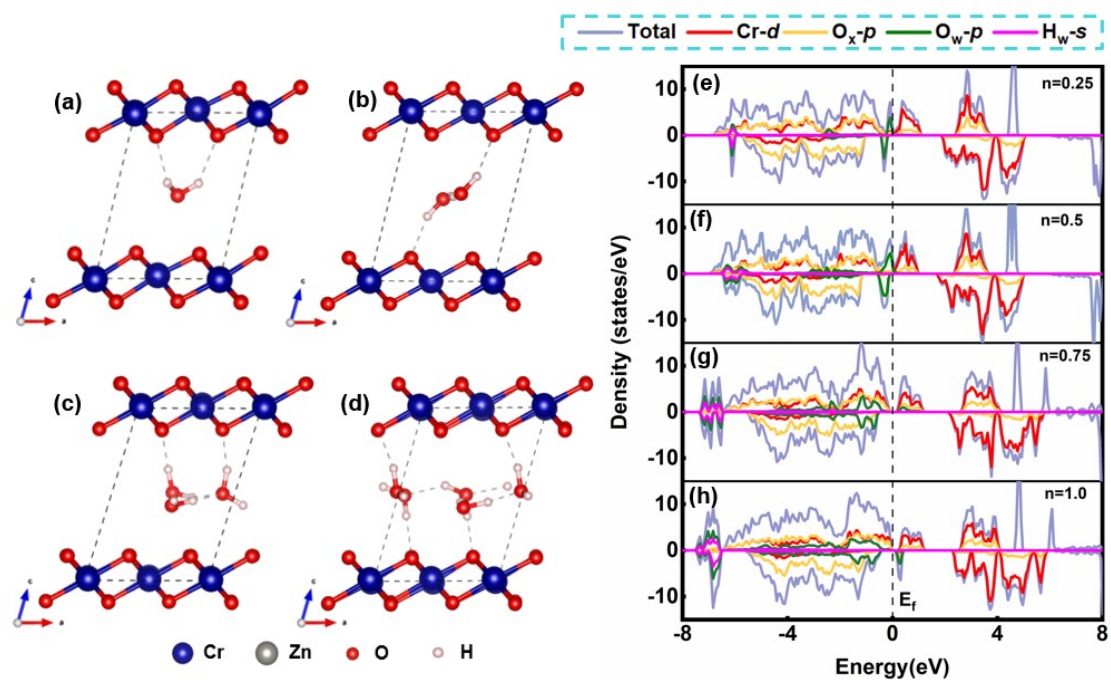

Fig. S9 The optimized pre-intercalation structure water model (CrO$_2$·nH$_2$O, (a-d)) and corresponding Density of states (e-h).
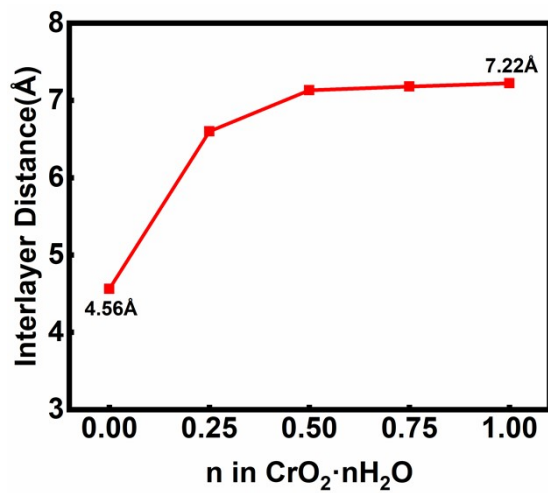

Fig. S10 The interlayer distance of CrO$_2$ electrodes after pre-intercalation into structural water(n=0.25~1.0)
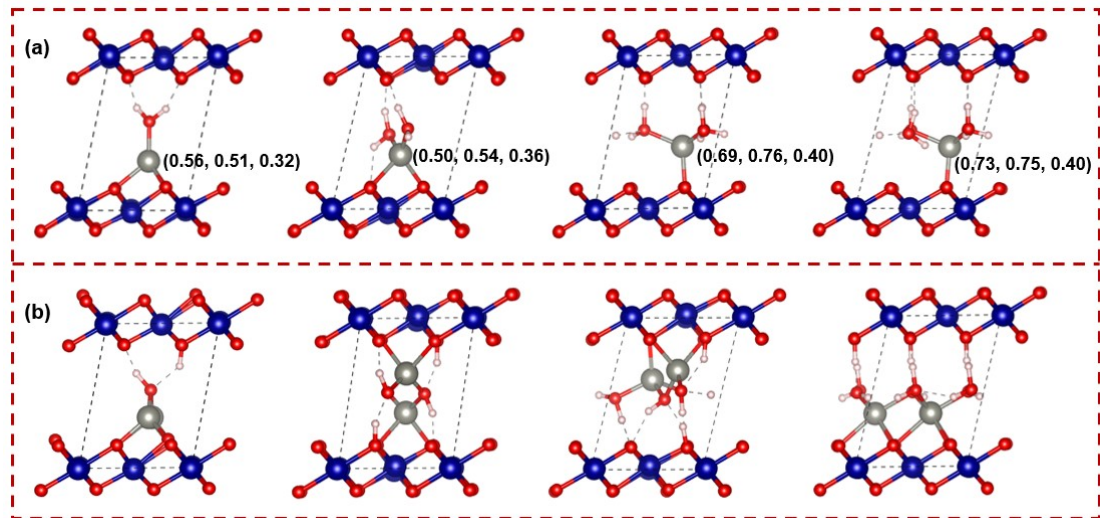
Zn insertion mechanism

Fig. S11 The structural configurations for Zn intercalation in (1×2×1) supercell of $CrO_2 \cdot nH_2O$ (n=0.25,0.5,0.75,1.0) with different Zn concentrations (a) c(Zn)=0.25; (b) c(Zn)=0.5.

H insertion mechanism

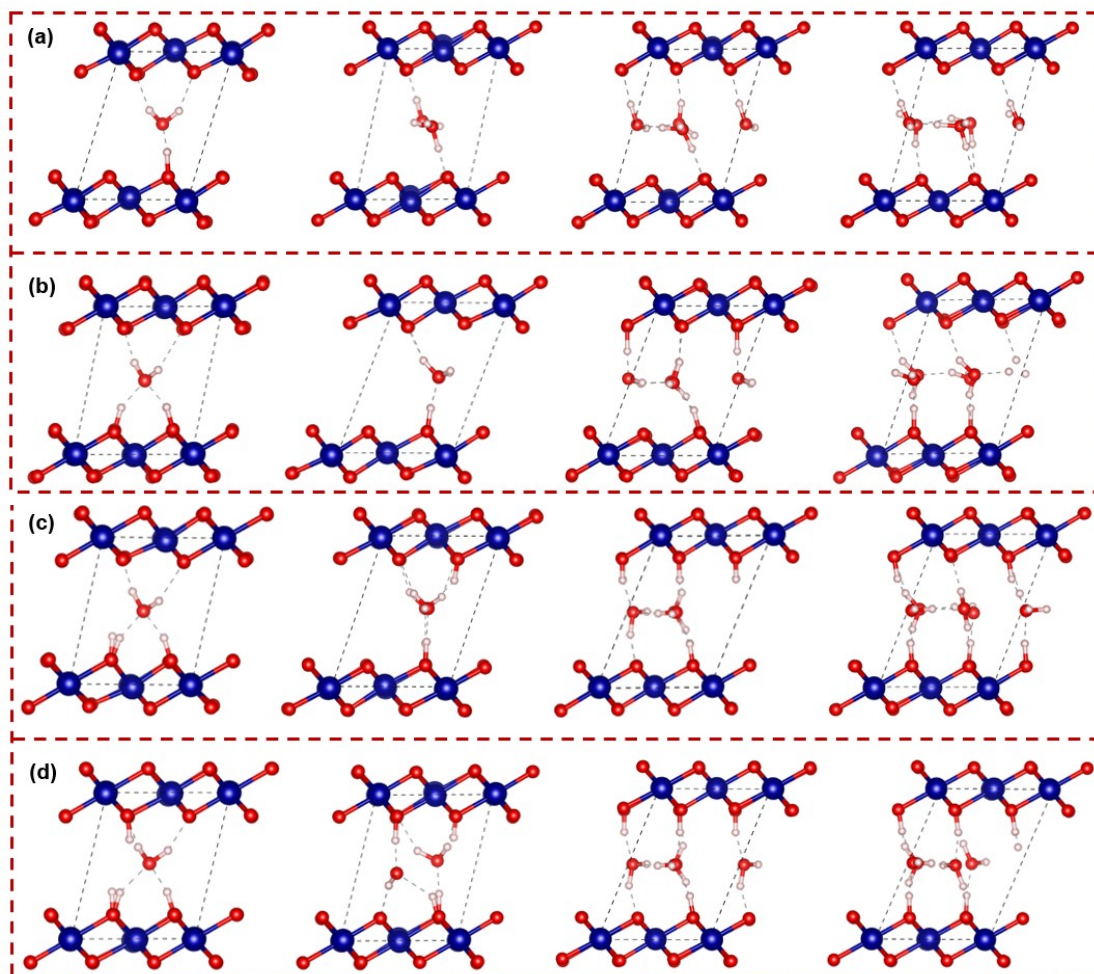Fig. S12 The structural configurations for H inserted in (1×2×1) supercell of $CrO_2 \cdot nH_2O$ (n=0.25,0.5,0.75,1.0) with different H concentrations (a) c(H)=0.25; (b) c(H)=0.5; (c) c(H)=0.75; (d) c(H)=1.0.
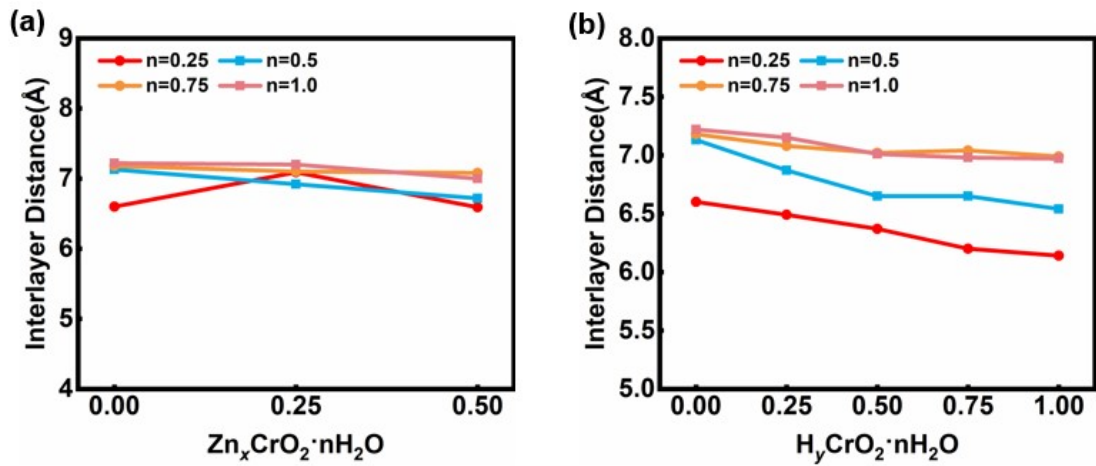
Fig. S13 The interlayer distance of $CrO_2 \cdot nH_2O$ at different insertion stages (a) Zn insertion mechanism; (b) H insertion mechanism.
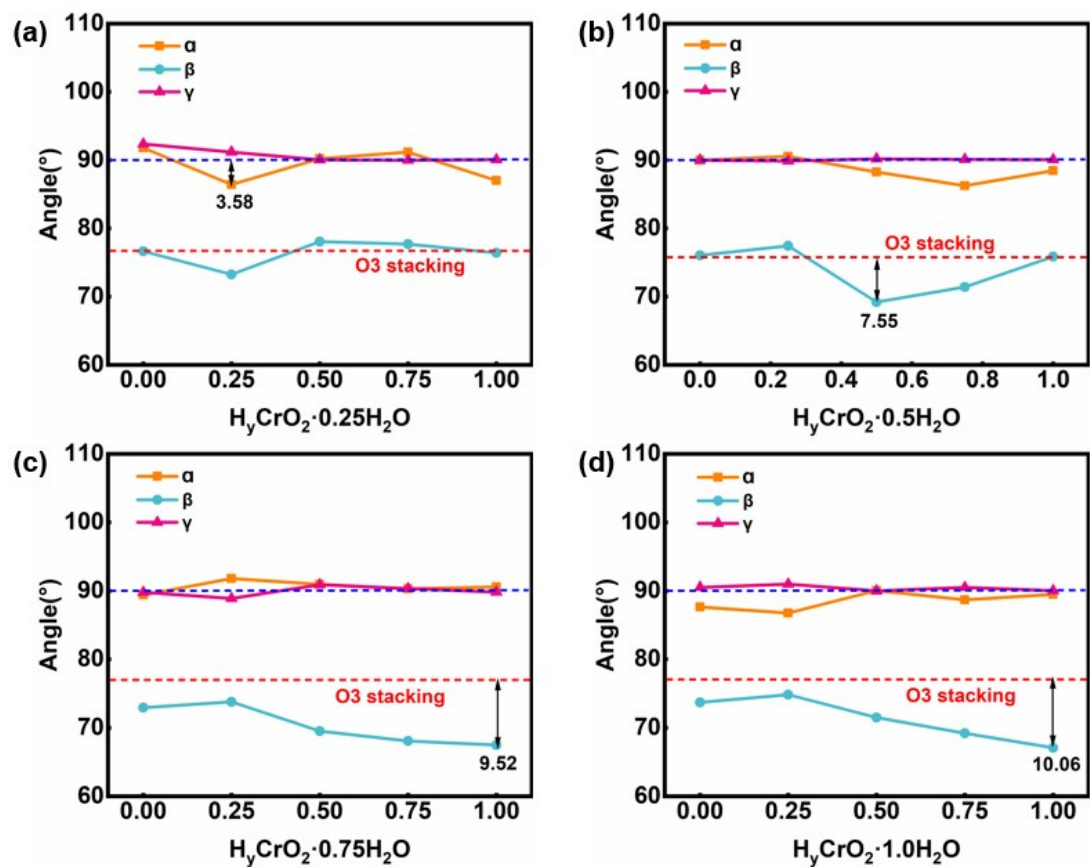
Fig. S14 The angle between the base vectors at different stages of H insertion in $H_yCrO_2 \cdot nH_2O$, (a) n=0.25; (b) n=0.5; (c) n=0.75; (d) n=1.0.
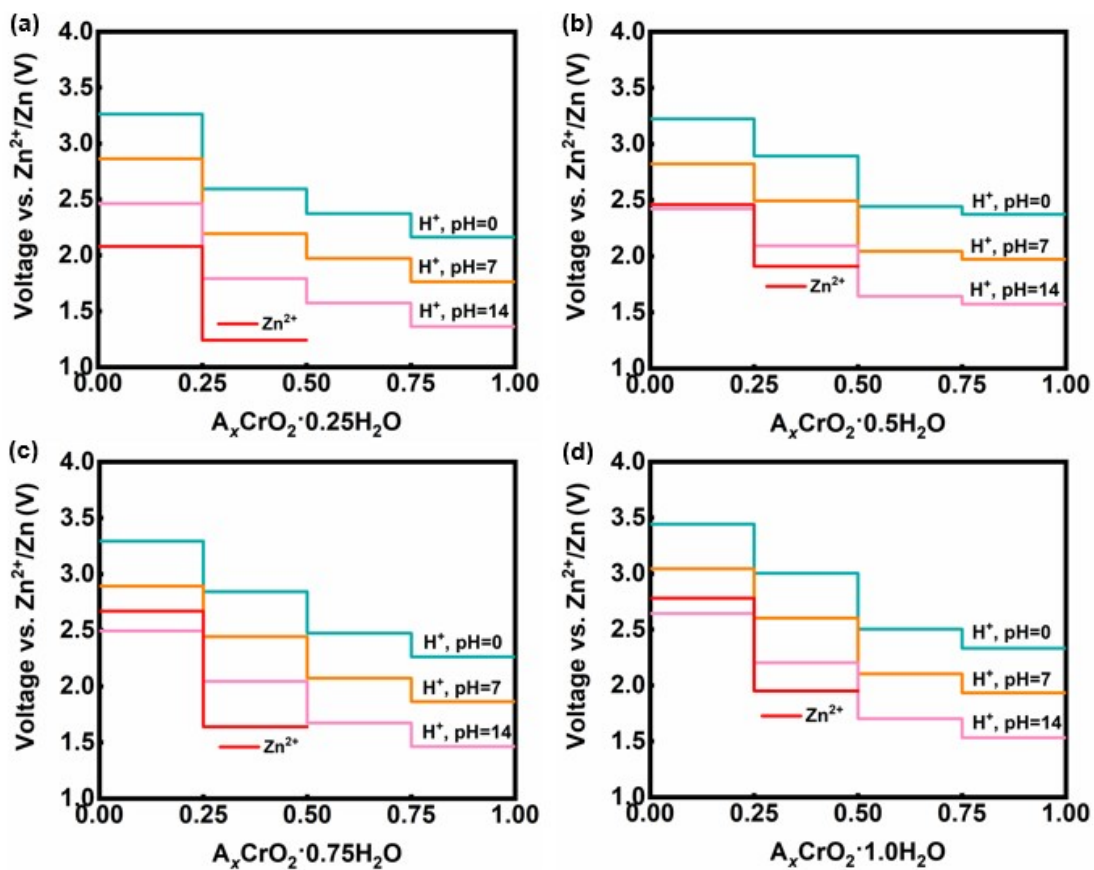
Fig. S15 Discharge curves of Zn^{2+} (red) and H^+ (based on different pH values) insertion/extraction process in $CrO_2 \cdot nH_2O$ (n=0.0~1.0).

H/Zn co-insertion mechanism

The most stable configuration

Fig. S16 The various optimized configurations of $H_{0.125}Zn_{0.125}CrO_2 \cdot 0.5H_2O$ (H/Zn co-insertion mechanism)

Table S2 Lattice parameters and volumes of $CrO_2 \cdot nH_2O$ and $Zn_xCrO_2 \cdot nH_2O$ configurations

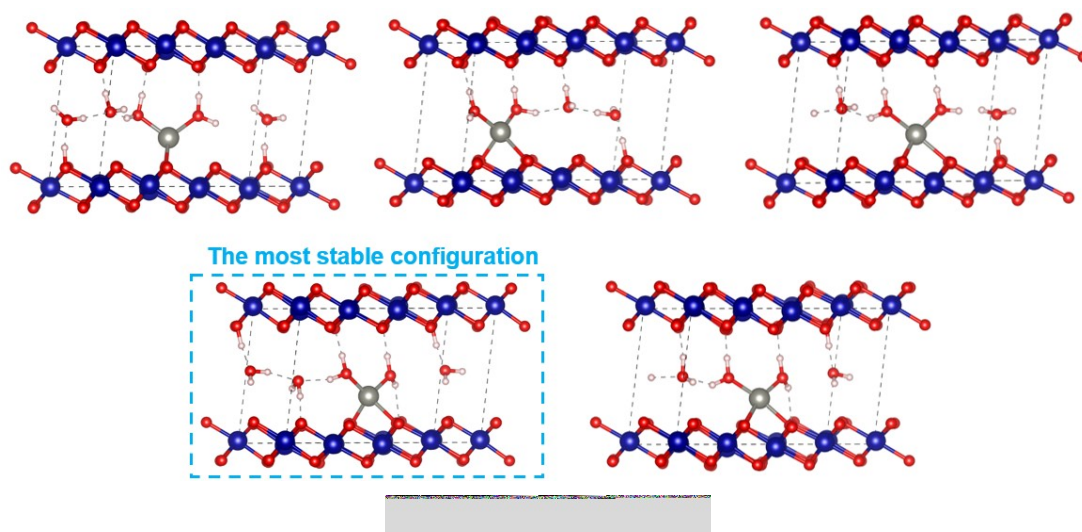| c(H₂O)	lattice parameter						volume
	a	b	c	α	β	γ	
	Å			o			Å³
0	5.048	5.828	4.853	90	69.72	90	133.929
0.25	5.004	5.924	6.836	91.79	76.64	92.36	196.962
x=0.25	5.143	5.92	7.372	93.65	78.01	89.83	219.075
x=0.5	5.214	6.012	6.828	84.43	78.66	89.77	208.820
0.5	5.184	5.677	7.45	90	76.055	90	212.807
x=0.25	5.133	5.909	7.192	84.94	76.55	90.96	211.188
x=0.5	5.183	6.058	6.853	90	82.44	90	213.344
0.75	5.145	5.832	7.52	89.39	72.93	89.78	215.576
x=0.25	5.107	5.954	7.336	88.70	77.07	89.42	217.417
x=0.5	5.241	6.051	7.317	86.63	76.24	91.55	224.818
1.0	5.207	5.821	7.560	87.63	73.69	90.50	219.693
x=0.25	5.137	5.955	7.308	87.95	78.23	91.53	221.476
x=0.5	5.235	6.061	7.235	90.03	76.47	89.99	223.186

Table S3 Lattice parameters and volumes of $CrO_2 \cdot nH_2O$ and $H_yCrO_2 \cdot nH_2O$ configurations

c(H₂O)	lattice parameter						volume
	a	b	c	α	β	γ	
	Å			o			Å³
0	5.048	5.828	4.853	90	69.72	90	133.929
0.25	5.004	5.924	6.836	91.79	76.64	92.36	196.962
y=0.25	5.042	5.963	6.878	86.42	73.25	91.18	197.449
y=0.5	5.105	6.008	6.536	90.21	78.07	90.04	196.144
y=0.75	5.187	6.053	6.414	91.17	77.69	89.98	196.736
y=1.0	5.267	6.093	6.411	87.02	76.43	90.06	199.719
0.5	5.184	5.677	7.45	90	76.055	90	212.807
y=0.25	5.155	5.795	7.159	90.56	77.44	89.87	208.743
y=0.5	5.146	5.962	7.224	88.26	69.19	90.19	207.033
y=0.75	5.244	5.998	7.143	86.25	71.40	90.11	212.420
y=1.0	5.261	6.079	6.788	88.46	75.84	90.08	210.399
0.75	5.145	5.832	7.52	89.39	72.93	89.78	215.576
y=0.25	5.124	5.85	7.472	91.79	73.79	88.88	214.901
y=0.5	5.124	5.998	7.427	90.95	69.52	90.88	213.819
y=0.75	5.201	6.04	7.578	90.29	68.06	90.32	220.825
y=1.0	5.253	6.101	7.558	90.58	67.47	89.82	223.739
1.0	5.207	5.821	7.560	87.63	73.69	90.50	219.693
y=0.25	5.179	5.829	7.476	86.75	74.84	90.97	217.392
y=0.5	5.209	5.941	7.445	90.03	71.49	90.00	218.542
y=0.75	5.239	6.024	7.498	88.68	69.20	90.49	221.109
y=1.0	5.269	6.108	7.604	89.48	67.09	90.02	225.444

References

[1] S.-H. Bo, X. Li, A.J. Toumar,andG. Ceder, Chemistry of Materials, 2016, 28, 1419-1429.

[2] X. Xia,andJ.R. Dahn, Electrochemical and Solid-State Letters, 2012, 15.